

RMP Colloquia

This section, offered as an experiment beginning in January 1992, contains short articles intended to describe recent research of interest to a broad audience of physicists. It will concentrate on research at the frontiers of physics, especially on concepts able to link many different subfields of physics. Responsibility for its contents and readability rests with the Advisory Committee on Colloquia, U. Fano, chair, Robert Cahn, S. Freedman, P. Parker, C. J. Pethick, and D. L. Stein. Prospective authors are encouraged to communicate with Professor Fano or one of the members of this committee.

Dynamics of earthquake faults

J. M. Carlson

Department of Physics and Institute for Theoretical Physics, University of California, Santa Barbara, California 93106

J. S. Langer

Institute for Theoretical Physics, University of California, Santa Barbara, California 93106

B. E. Shaw

Institute for Theoretical Physics, University of California, Santa Barbara, California 93106 and Lamont-Doherty Earth Observatory, Columbia University, Palisades, New York 10964

The authors present an overview of ongoing studies of the rich dynamical behavior of the uniform, deterministic Burridge-Knopoff model of an earthquake fault, discussing the model's behavior in the context of current seismology. The topics considered include: (1) basic properties of the model, such as the distinction between small and large events and the magnitude vs frequency distribution; (2) dynamics of individual events, including dynamical selection of rupture propagation speeds; (3) generalizations of the model to more realistic, higher-dimensional models; and (4) studies of predictability, in which artificial catalogs generated by the model are used to test and determine the limitations of pattern recognition algorithms used in seismology.

CONTENTS

I. Introduction: The Dynamical Richness of Seismic Phenomena	657
II. The Model: Complex Behavior from a Simple Dynamics	659
III. Properties of the Uniform Burridge-Knopoff Model: Small and Large Events	661
IV. Ruptures: Numerical Observations and Analytical Solutions	663
V. Higher Dimensions: Moving Towards More Realistic Models	665
VI. Predictability: Forecasting the Next Large Earthquake	667
Acknowledgments	669
References	669

I. INTRODUCTION: THE DYNAMICAL RICHNESS OF SEISMIC PHENOMENA

Two trends that have characterized much of modern theoretical physics are an increased capability for dealing with complex systems and an increased interest in topics that traditionally have been the property of other disciplines. Investigations that fall into the latter category can be especially rewarding, but it is necessary to "take stock" every so often to make sure that one is really working along lines that are meaningful. The present article is a "stock-taking" with regard to our recent investigations of the dynamics of a simple model of an earthquake fault.

The earthquake problem certainly satisfies our criteria for trendiness both in complexity and interdisciplinarity. A wide variety of points of view have been taken in recent years by geologists, seismologists, mechanical en-

gineers, mathematicians, and physicists. Ours has been a comparatively narrow one. We have focused on what we believe to be the simplest nontrivial model of a single segment of an earthquake fault and have examined its dynamic properties. As we describe below, our results have been interesting enough to encourage us to extend our investigations to more practical applications of the model. Before outlining these results, however, we shall provide a broader context for them by devoting a few paragraphs to some general aspects of the earthquake problem. For a more complete discussion see, for example, Scholz (1990).

One spectacular feature of earthquakes is the enormous range of scales over which they occur. The distribution of sizes of seismic events is observed to be a power law over more than ten orders of magnitude (though the exponent may vary somewhat across this range). This power-law distribution of event sizes, known as the Gutenberg-Richter law (Gutenberg and Richter, 1954), is one of the most fundamental observations in seismology. Its explanation remains an outstanding question in the earth sciences. Two possibilities have been the topic of much debate recently. One point of view is that geometric and material irregularities in the earth dominate the behavior, and it is therefore "quenched disorder" which underlies the answer. An alternative point of view is one in which complexity arises primarily as a consequence of dynamical instabilities. In this case, nonuniformities evolve as the system evolves, with no *a priori* fixed inhomogeneities or stochastic forcing. Whether the earth is operating in one regime or another

or in some combination remains an open and fundamental question.

Typically, earthquakes occur in the upper ten kilometers or so of the earth's crust. They arise as a consequence of frictional instabilities that cause stress, accumulated by large-scale plate motions over periods of hundreds of years, to be relieved in sudden stick-slip events. In other cases, deep in the crust, for example, frictional properties may allow stable sliding, so that strain is relieved smoothly and aseismically. A different class of events, known as "deep earthquakes," occurs along subducting plates, at depths of hundreds of kilometers. The basic physical processes that are responsible for deep earthquakes are not well understood, but these events are suspected to be caused by the plates undergoing phase changes at the high temperatures and pressures associated with large depths.

The motions of tectonic plates are driven by large-scale convective flows in the mantle. These flows take place on length scales of thousands of kilometers with turnover times of hundreds of millions of years; thus characteristic speeds are of the order of centimeters per year. Understanding these inner motions of the earth is yet another important object of research, carried out these days primarily by geophysicists and fluid dynamicists (see, for example, Glatzmaier *et al.*, 1990). These inner motions may be intrinsically chaotic; for example, material from the earth's core may be brought to the surface by intermittent plumes that rise through the mantle. Nevertheless, the large-scale convection is so slow and powerful that it may be thought of as providing a constant external driving force for seismological purposes.

Of more direct seismological interest is the manner in which the inner flows couple to the brittle outer layers, thereby driving relative motions of the plates and producing the intricate patterns of cracks that we know as earthquake faults. One of the main themes of modern seismology is the use of basic principles of fracture mechanics for understanding the way in which stresses applied to the crust have produced the various kinds of faults that are known to exist (see, for example, Scholz, 1990). A recent trend has been to ascribe fractal properties to the complex arrays of fault segments that occur in the regions where major plates come into contact with each other (Kagan, 1982; Barriere and Turcotte 1991; Knopoff, 1993; Sahimi *et al.*, 1993). Why these patterns have the geometric properties that are observed, and what may be the implications of these geometries for predicting the frequencies and sizes of seismic events are outstanding research questions. It may be, for example, that each segment of a complex pattern of faults undergoes its own characteristic cycle of earthquakes with only relatively weak coupling to its neighbors. If so, then the statistical distribution of earthquake magnitudes will be determined primarily by the statistics of fault segments—the disorder is quenched into the system—and the most important concepts in theoretical seismology will be geometric in nature.

A hypothesis that attempts to explain the observed

geometric irregularities within a dynamical framework is known as "self-organized criticality" (Bak *et al.*, 1987; Chen *et al.*, 1991). The idea is that many systems in nature, the earth's crust, for example, are driven by external forces in such a way that they are always at or near a threshold of instability. Tectonic plates retain their integrity or remain locked to one another until the stresses that are imposed upon them are partially relieved by events such as fault formation or earthquakes, but the stresses begin to rise toward threshold again as soon as an event is over. It seems possible that systems that operate persistently near a threshold of instability are in some way like thermodynamic systems near critical points. If, as in critical phenomena, some length or time scale is diverging near threshold, then fluctuations may occur over anomalously broad ranges of size or duration. So far as we know, there does not yet exist a systematic mathematical definition of a state of self-organized criticality. The hypothesis remains an intriguing conjecture that has served to stimulate a variety of theoretical investigations including our own. As we shall see, the earthquake model that we have studied does exhibit some features of a critical system, but there are other respects in which it differs markedly from the hypothetical ideal.

The principal result of our studies is that a spatially uniform block and spring model—the one-dimensional "Burrige-Knopoff model" (Burrige and Knopoff, 1967) without built-in irregularities or external noise—is a deterministically chaotic dynamical system whose behavior is similar in some important ways to the behavior of real earthquake faults. In particular, the model exhibits a broad spectrum of small to moderately large, spatially localized, earthquakelike events, which move stress from one location to another but do very little to relieve stress in the system as a whole (Carlson and Langer, 1989a, 1989b; Carlson *et al.*, 1991). It also exhibits spatially extended "great events" in which strong slipping pulses arise at "epicenters" and propagate along the fault, thereby unloading the stress on large segments of the system. The sizes of the smaller events obey a power-law distribution much like the Gutenberg-Richter law. The great events recur irregularly on roughly a loading period—the time necessary for the tectonic forces to build stress up to the breaking point—and their frequency as a function of magnitude is not generally a simple extension of the power-law distribution for the smaller events (Carlson, 1991a). This rich pattern of apparently realistic behavior emerges from a model with essentially only one adjustable, material-dependent parameter, and with no externally imposed spatial or temporal structure.

We have used the term "apparently" here because this is, at best, a model of a single isolated fault or fault segment. The intrinsic dynamic properties of single faults are not known with precision, and many aspects of the subject remain controversial. The catalogs of seismic events on which the Gutenberg-Richter law is based almost always pertain to large regions containing many faults; and the statistics of large characteristic events on

single faults are necessarily very poor because the recurrence times for such events are usually centuries or longer (Nishenko and Buland, 1987). The manner in which slip propagates in this model (Langer and Tang, 1991; Langer, 1992; Langer, 1993; Langer and Nakanishi, 1993; Myers and Langer 1993a) looks very much like the conjectured "Heaton pulse" (Heaton, 1990). However, much work remains to be done before we know whether this pulse is actually the normal mechanism for slip in large earthquakes and, if so, whether the pulse that occurs in the Burridge-Knopoff model has anything in common with the real one.

Thus there are large uncertainties in our understanding of seismic phenomena in the earth, and the uniform Burridge-Knopoff model is far from being an accurate representation of even the simplest faults. (It does not even contain a mechanism for aftershocks.) What, then, can we say about meaningful accomplishments and future prospects for research along these lines? In large part, this article is devoted to answering that question. As in any theoretical project, much of the answer is that the insight gained from modelistic studies can be helpful in interpreting real data and in developing more realistic models. After a brief introduction to the simplest version of this model in Sec. II, we describe several such interpretations and extensions that we believe are particularly promising: the distinction between localized and delocalized events, pulse propagation, and some higher-dimensional models, which include either patterns of slip on the fault plane or elastic deformations normal to that plane. These topics are discussed in Secs. III–V.

We conclude in Sec. VI with an introduction to what is—for physicists, at least—an unconventional use of physical models. The idea is to use this model as a tool for developing objective techniques for earthquake prediction. As mentioned above, the Burridge-Knopoff model is highly idealized, but it has two especially important features: it is intrinsically and deterministically chaotic—and therefore technically "unpredictable"; and it produces a clear distinction between frequent small events and the rare large ones about which we would like to be warned in advance. Thus this model and its more realistic extensions ought to provide practical, quantitative tests for the validity of prediction schemes.

II. THE MODEL: COMPLEX BEHAVIOR FROM A SIMPLE DYNAMICS

We start by considering the simple model of an earthquake fault illustrated schematically in Fig. 1. Here, two adjoining elastic plates are being pushed together and forced to move in opposite directions along their line of contact. The corresponding compressive and shear stresses are applied at some distance from this "fault" line. The plates are "stuck" to each other at the fault but, whenever the threshold for sticking friction is exceeded by the local shear stress, the plates move in an earthquakelike slipping event.

This model contains three essential ingredients:

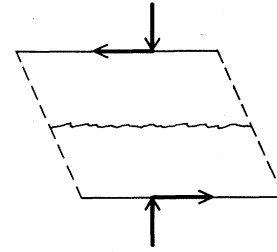


FIG. 1. Schematic representation of a lateral fault embedded in an elastic medium. Shear and normal stresses, applied far from the interface between the homogeneous elastic plates, and are relieved by sudden slipping motions, which occur when the friction threshold is exceeded.

- (1) A mechanism for loading the system, i.e., for applying the shear stress.
- (2) Mechanisms for storing the elastic energy associated with both the compressive and the shear stresses.
- (3) Stick-slip friction action between the plates along the fault line. It is essential that this be a velocity-weakening friction. That is, once slipping begins, the frictional force decreases with increasing slipping speed. The resulting dynamic instability is responsible for almost all of the interesting properties of this class of models.

We also insist that this be a fully deterministic, dynamical model. The benefit of studying a dynamical system as opposed to, say, a cellular automaton is that we can more easily identify characteristic length and time scales with the corresponding parameters in the laboratory or the earth. Moreover, our physical intuition leads us to believe that deterministic inertial dynamics is an essential ingredient of a theory of earthquakes.

All of these ingredients are contained in the uniform Burridge-Knopoff model, which is illustrated in Fig. 2. The model consists of a one-dimensional chain of blocks and springs that is pulled slowly across a rough surface. Comparing this simple mechanical model with the idealized fault illustrated in Fig. 1, we see that the blocks represent a discretization of one side of the fault in which the fault line is the contact surface between the blocks and the fixed rough surface on which they slide, and the

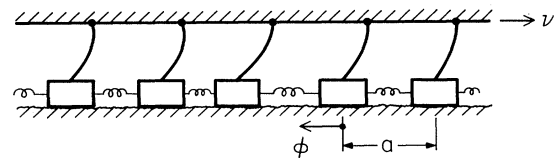


FIG. 2. The one-dimensional uniform Burridge-Knopoff model represents the finite-difference approximation to Eq. (1). The system consists of a uniform chain of elastically coupled masses, located at positions $U(x, t)$ along the x axis, which we imagine to be the axis of a lateral fault. Each block is connected to its two neighbors by harmonic coil springs and is pulled individually forward through an elastic leaf spring that moves at constant velocity v . The ratio of the coil spring strength to the leaf spring strength is $(\xi/a)^2$, where a is the equilibrium block spacing. The key nonlinearity leading to complex behavior is the friction law ϕ illustrated in Fig. 3.

coil springs and leaf springs, respectively, represent the linear elastic response of the plates to compression and shear. If the blocks were able to slide without friction on the lower plate, disturbances would propagate indefinitely like waves with a speed determined by the masses and spring constants.

However, the velocity-weakening stick-slip friction at the interface between the blocks and the rough surface changes the character of the motion dramatically. The system is driven by pulling the upper surface slowly forward at some constant velocity. At most times, the blocks remain stationary on the rough lower surface, held there by the sticking friction while the leaf springs are stretched by the driving force. Note that we have placed the middle block in Fig. 2 slightly to the left of center so that the forces pulling it to the right are slightly greater than those acting on its neighbors. As a result, the forces acting on this block will be the first to reach the threshold for sticking friction. When this happens, the block will slip forward, increasing the forces on the neighboring blocks and possibly causing them to move as well. In this way, the motion triggered by the instability of a single block may induce an event—an “earthquake”—in which many blocks move forward in a complex slipping pattern.

The continuum limit of the one-dimensional Burridge-Knopoff model is defined by the partial differential equation

$$\ddot{U} = \xi^2 \frac{\partial^2 U}{\partial x^2} - U - \phi(\dot{U}) + \nu t. \quad (1)$$

Conversely, the blocks and springs in Fig. 2 represent the elementary finite-difference approximation to Eq. (1). Equation (1), or its discretized version, is Newton’s law of motion in an almost dimensionless form. The function $U(x, t)$ is the time-dependent displacement of the material at position x along the fault. The inertial term is on the left-hand side. The first two terms on the right are the (linear) compressional and shear forces, respectively, and $\phi(\dot{U})$ is the velocity-dependent friction. Finally, νt is the driving force; that is, ν is the dimensionless loading rate. Note that, in contrast to the original work by Burridge and Knopoff and many subsequent investigators, our version of the model is completely uniform. All of the physical elements—masses, springs, friction forces—are identical to one another, and we shall introduce no external noise or other stochastic ingredients.

We have scaled Eq. (1) in such a way that the largest possible earthquake, in which the system slips forward uniformly through one half period of the simple harmonic motion determined by the shear force, has a duration $\Delta t = \pi$ and a corresponding slip distance $\Delta U = 2$. In other words, our time t is measured in units of a characteristic slip time (sometimes called the “rise time”), which, in the earth, is of the order of seconds. Our displacements U are measured in units of a characteristic slip distance, which usually is of the order of meters.

The dimensionless loading rate ν is measured in units of the characteristic slipping speed. Because the latter is

of the order of meters per second, and geological loading rates are of the order of centimeters per year, ν is of order 10^{-8} or less. An equivalent way of saying this is that geological loading periods—the times required for the tectonic forces to build back up to the slipping threshold after a very large event—are generally of the order of centuries in real time, and are of the order $\nu^{-1} \approx 10^8$ in our dimensionless units. This very large difference between rise times and loading periods means that earthquakes, both in the earth and in our model, are sharply defined events that can be observed and catalogued unambiguously.

In order to avoid confusion between displacement U and position x (which both have the dimensions of length but which scale quite differently), we have chosen to leave x in dimensional units rather than further simplifying Eq. (1) by writing x in units of ξ . The length ξ is the distance traveled by a sound wave in a slipping time, and thus is of the order of ten kilometers. This length necessarily is the same as the thickness of the seismogenic layer of the earth’s crust; it is the only length available for setting the frequency of the slowest harmonic mode in the system, that is, for determining the coefficient (unity in our notation) of $-U$ in Eq. (1). Because time is dimensionless, we shall also speak of ξ as a velocity. The one remaining length scale in the problem is the block spacing a , which is shown in Fig. 2, but which disappears in the continuum limit implicit in Eq. (1). We shall see that a plays a crucial role as a short-distance or, equivalently, high-frequency cutoff; that is, Eq. (1) is not by itself a mathematically well posed differential equation.

The only nonlinearity in Eq. (1) is contained in the slip-stick friction law $\phi(\dot{U})$, which we show schematically in Fig. 3. An elementary mass point along the fault—that is, a “block” in Fig. 2—remains stuck at $\dot{U} = 0$ until the force on it exceeds some threshold, which we have scaled to unity. When a block starts to slide, the frictional resistance to its motion decreases at a rate 2α . The quantity α is (very nearly) the only dimensionless parameter that contains information about the constitutive properties of the material; it is the ratio of the charac-

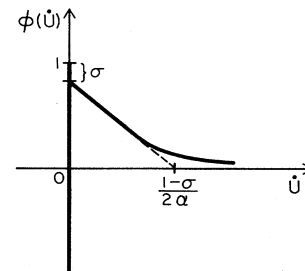


FIG. 3. The velocity-weakening slip-stick friction law $\phi(\dot{U})$. Sticking friction satisfies $\phi(0) \leq 0$, while slipping friction decays monotonically to zero from the initial value $\phi(0^+) = 1 - \sigma$, with initial slope equal to -2α . This initially negative slope gives rise to the intrinsic instability, which ultimately leads to complex behavior. Note that the form of Eq. (1) is invariant (upon resetting the zero of displacement) with respect to addition of a constant to the high-speed friction.

teristic slipping speed (meters per second) to a speed that characterizes the velocity-weakening property of the friction law. Thus, if α is large, the fault quickly becomes “slippery” once motion begins, and this motion is strongly unstable. Conversely, if α is small, the fault remains relatively “sticky” during motion, and the instability is weak. It is important to note that, because the elastic forces in Eq. (1) are all linear, we can reset the zero of $\phi(\dot{U})$ simply by shifting the zero of U ; thus, without loss of generality, we have let $\phi(\dot{U})$ vanish for large \dot{U} , and we also have let the multivalued quantity $\phi(0)$ be as large and negative as is necessary to prevent backsliding. That is, we constrain the motion so that $\dot{U} \geq 0$.

For the numerical calculations reported here, we have chosen

$$\phi(\dot{U}) = \begin{cases} (-\infty, 0], & \dot{U} = 0, \\ \frac{1-\sigma}{1+2\alpha\dot{U}/(1-\sigma)}, & \dot{U} > 0. \end{cases} \quad (2)$$

The “onset parameter” σ is the acceleration of a block at the instant when slipping begins. We have introduced σ primarily as a technical device that allows us to study the limit $\nu \rightarrow 0$. In the absence of σ , events begin indefinitely slowly in that limit, which obviously is inconvenient for numerical purposes. Further, it seems improbable that the order of magnitude of the very small driving rate ν should influence the dynamics of events on a completely different scale. In fact, if there is a separate nucleation process leading up to an event, then a finite σ , which provides an initial “kick,” may be a realistic effect. With nonzero σ and vanishingly small ν we need not carry out explicit time integrations between slipping events, and thus we are able both to use a geologically realistic loading rate and to study the system for very large numbers of loading cycles. Accordingly, we have used small values of σ , usually 10^{-2} , for generating large artificial earthquake catalogs.

In summary, the uniform Burridge-Knopoff model is fully determined by only the following dimensionless, system-dependent parameters. Principally, there is the friction parameter α , which determines all of the most important features of earthquakes, especially the qualitative features of their frequency distribution as a function of magnitude. In addition, there is the ratio ξ/a , which diverges in the continuum limit and determines the range of sizes over which different behaviors are seen. As might be expected, ξ/a determines the small-magnitude cutoff of the frequency distribution. Interestingly, it also determines the upper cutoff for great events in very large systems and, in addition, determines the propagation speeds and widths of rupture pulses in such events. The loading rate ν and the onset parameter σ may both be thought of as being arbitrarily small. (They do, however, play roles in distinguishing localized from delocalized events.) The only other parameter that plays any role is the size of the system, that is, the number of “blocks.” There are some situations in which it is useful to consider

small systems; for example, it may be interesting to simulate the behavior of short fault segments. For present purposes, however, we shall consider only systems that are indefinitely large; then, because there is a finite cutoff μ^* for the largest events, in large enough systems, the system size is irrelevant.

III. PROPERTIES OF THE UNIFORM BURRIDGE-KNOPOFF MODEL: SMALL AND LARGE EVENTS

In our earliest investigations of the uniform Burridge-Knopoff model, we have taken advantage of the ease with which Eq. (1) can be integrated numerically to generate long and accurate artificial catalogs of seismic events. Using only a modest workstation, we have been able to obtain the geological equivalent of tens of thousands of years of data, which, unlike real seismological data, are free of observational errors or uncertainties. Our initial goal in this effort was simply to find out whether so elementary a model might behave in a way that is at all similar to the behavior of a real earthquake fault. We shall describe a more ambitious and speculative use of these artificial catalogs in Sec. VI.

We generally have carried out our numerical solutions

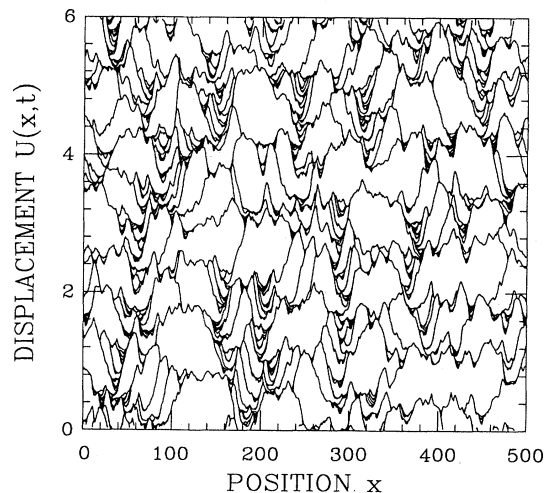


FIG. 4. The displacement $U(x,t)$ for a typical sequence of events, plotted immediately after each event as a function of position x along the fault. The lowest contour corresponds to the earliest configuration, taken after the initial transient period has passed and the system has reached a statistically steady state. Subsequent curves correspond to the sequence of stuck configurations observed as Eq. (1) is integrated forward in time. The seismic moment of each event corresponds to the area swept out between adjacent curves. In spite of the underlying homogeneity of the system, the behavior is quite complex. While the system is technically chaotic, it also displays short-term “patterns,” which can be used for predictive purposes. In particular, the smaller events tend to cluster in the roughly parabolic minima, preparing a nucleation zone for the triggering of a future large event. Here we have taken $\sigma=0.01$, $\alpha=1.2$, $\xi/a=2.0$, and $N=500$. In the more generic case of $\alpha > 2$ the small events account for even less of the net displacement than for the parameter values taken here.

of Eq. (1) by choosing some small inhomogeneity in the initial displacements and then allowing the system to evolve until it reaches a statistically steady state. A typical evolution of the system, beginning after the initial transient has passed, is illustrated in Fig. 4. Here, we plot a sequence of “stuck” configurations $U(x, t)$ as functions of position x . A new curve is drawn after each event, which begins when the force on some block exceeds the static friction threshold and concludes when the entire system comes to rest. Clearly, the motion shown here is very complex. Indeed, it is technically chaotic in the sense that nearby configurations move apart, on average, exponentially fast. Events occur over a wide range of sizes and, while the eye can discern certain patterns, the system is not behaving in a periodic or quasiperiodic manner.

The most striking feature of Fig. 4 is the distinction between small and large events. The smaller events are by far the most numerous. They tend to occur in clusters and to fill in local minima in the displacement curve $U(x, t)$ where many blocks are close to their slipping thresholds. The large events are much less frequent but dominate the net motion of the system; they cover most of the area in Fig. 4.

In analogy to the seismological convention, we define the seismic moment M to be the integrated slip, that is, the area swept out by an event in Fig. 4. We further define the “magnitude” of an event¹ to be $\mu = -\ln M$, and we denote the differential magnitude vs frequency distribution by $R(\mu)$. A typical frequency distribution $R(\mu)$ is shown in Fig. 5 for a sequence of events like that shown in Fig. 4, but for a much larger system (over 8000 blocks), a much larger number of loading cycles (over 100), and slightly different values of the parameters. Here we see that the sharp distinction between small and large events that is visible in Fig. 4 is also manifest in the statistical properties of the system. The small events, with magnitudes between some lower bound μ_1 determined by the block size and a crossover value $\bar{\mu}$, are distributed according to our analog of the classic Gutenberg-Richter law:

$$R(\mu) = Ae^{-b\mu}, \quad (3)$$

with b very nearly to unity for large enough α . [For “stickier” faults with α less than about 2, smaller values of b are obtained (Carlson and Langer, 1989b; Vascon-

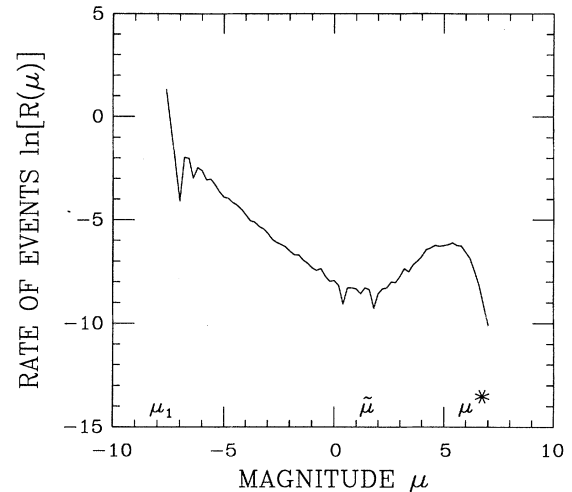


FIG. 5. Magnitude vs frequency distribution for the uniform Burridge-Knopoff model. Here we have taken $\sigma=0.01$, $\alpha=2.5$, $\xi/a=6$, and $N=1500$. The most striking feature is the statistical distinction between small and large events, marked by the crossover $\bar{\mu}$, which corresponds to an upper bound on the size of the small clustering events in Fig. 4. A more detailed numerical study of the scaling of this distribution reveals an interesting sensitivity of the magnitude of the largest events to the presence of the short-wavelength cutoff a (Carlson *et al.*, 1991). In particular, for N sufficiently large, both the magnitude of the crossover $\bar{\mu}$ and largest event μ^* are independent of N . However, while $\bar{\mu}$ is independent of a , we find that μ^* increases as the mesh becomes finer, scaling roughly as $\mu^* \sim \ln(\xi^2/a)$.

celos *et al.*, 1992)]. The large events, with magnitudes greater than $\bar{\mu}$, occur at a rate that is higher than the extrapolated “ $b=1$ ” law, and their distribution cuts off sharply at a magnitude μ^* , which, for large enough systems, is independent of the system size.

All of the above features of Fig. 5 are qualitatively similar to behavior that is often—but not always—observed seismologically. The similarity pertains only to data taken for a single fault system and not to catalogs that combine data from many different faults with qualitatively different characteristics (see, for example, Scholz, 1990). The interpretation of earthquake catalogs remains somewhat controversial, and we shall not try to discuss in any detail the current state of those debates. In brief, it appears that smaller events on real faults, with Richter magnitudes roughly in the range 1–6, are in some sense self-similar and obey some scaling distribution, but probably with b values (as defined here) appreciably smaller than unity (Pacheco *et al.*, 1992). The overabundance of large events for single faults is difficult to observe directly because repeat times are of the order of hundreds of years. However, the distribution of smaller events, even if extrapolated to Richter magnitudes 8 or 9, appears to account for only a small fraction of the total slip on individual faults. Thus there is indirect geological evidence that most of the displacement and energy release occurs during very large “characteristic” earthquakes whose recurrence frequency lies well above the extrapolated scal-

¹The usual Richter magnitude is measured on a \log_{10} scale and for historical reasons is defined in terms of the response of a specific instrument to ground motion. The magnitude μ , which we use, is most clearly related to a quantity referred to as the moment magnitude (Hanks and Kanamori, 1979), which is based on estimates of the total slip. The wide range of sizes of seismic events and the necessarily remote means by which events are detected have led to the development of numerous magnitude scales.

ing distribution (Schwartz and Coppersmith, 1984; Davison and Scholz, 1985; Wesnousky, 1993; for a different interpretation see Hanks, 1992).

The distinction between large and small—or delocalized and localized—events is probably the most significant new physical insight to emerge from this study. We can understand what is happening, roughly, as follows. Consider a zone along the fault of width Δx in which all of the blocks are at or very near their slipping thresholds; that is, in Eq. (1) $\xi^2 \partial^2 U / \partial x^2 - U = 1$. When we linearize Eq. (1) about a configuration of this kind, we find that an initially sharp slipping pulse propagates at speed ξ and grows like $e^{\alpha t}$ as it picks up stored elastic energy within the zone. If triggered by the natural evolution of the system, the initial amplitude of such a pulse would be proportional to the onset parameter σ . The delocalization criterion is simply the condition that, when this growing pulse reaches the edge of the zone where the blocks are further away from their slipping thresholds, its strength has become sufficient to dislodge those blocks and thus sustain its motion. Because the pulse propagates for a time of order $\Delta x / \xi$ within the zone, the width of the smallest slipping zone that can nucleate a delocalized event must be proportional to $(\xi / \alpha) \ln(1 / \sigma)$.

A more careful analysis (Carlson and Langer, 1989b; Carlson, *et al.*, 1991) yields the delocalization length:²

$$\tilde{\xi} \approx \left(\frac{2\xi}{\alpha} \right) \ln \left(\frac{4\xi^2}{\sigma a^2} \right). \quad (4)$$

Integrating the displacement associated with an event of size $\tilde{\xi}$, we obtain the crossover magnitude

$$\bar{\mu} \approx \ln \left(\frac{2\xi}{\alpha} \right), \quad (5)$$

which is consistent with the minimum in Fig. 5.

For realistic values of the parameters, the crossover length $\tilde{\xi}$ is of the order of tens of kilometers. Because $\tilde{\xi}$ scales like ξ , it will generally be of the same order of magnitude as the thickness of the seismogenic layer, even in this one-dimensional model where earthquakes have no structure in the fault plane. The length $\tilde{\xi}$ can be viewed as a correlation length for the model because it defines an upper bound on the length scale over which small events tend to cluster. Events that occur on length scales smaller than $\tilde{\xi}$ tend to smooth the system, thereby preparing an increasingly large triggering zone for a coming large event. On the other hand, because of the

stick-slip instability, events that occur on length scales larger than $\tilde{\xi}$ tend to roughen the system, leading to later sequences of smaller events. This interplay between small and large events implies that an understanding of the dynamics of the large events will be necessary in order to calculate the scaling distribution for the smaller events. As yet, we have found no convincing derivation of the “ $b=1$ ” law for the uniform Burridge-Knopoff model.

Note that the block spacing a appears explicitly on the right-hand side of Eq. (4); this is our first indication that the short-wavelength cutoff is playing an important role in the dynamics of this system. Interestingly, our numerical simulations indicate that a plays a role in determining the size of the largest event μ^* as well (see Fig. 5). We shall see in the following section that a shows up again in the pulse-propagation problem.

IV. RUPTURES: NUMERICAL OBSERVATIONS AND ANALYTICAL SOLUTIONS

Two unavoidable facts make direct observation of earthquake ruptures nearly impossible. First, most earthquakes occur well below the surface of the earth, and, second, earthquakes occur suddenly, at irregular time intervals, making it difficult for the observer to be at the right place at the right time. Thus, instead of direct measurements, seismologists measure the shaking produced at the earth’s surface at remote stations, and try to invert the signal to infer the motions at the source. However, the inversion problem is intrinsically complicated. For example, the effects of inhomogeneities in the crust on the attenuation of radiated waves are not fully understood, making it difficult to separate the effects that are due to the source from those due to the path. In addition, the problem of inverting an array of seismograms to deduce the source motion is underdetermined, since it involves reconstruction of motions in two space dimensions and one time dimension using a finite number of one-dimensional time series collected at different stations. Theoretical models thus play a crucial role in the inversion process.

In the Burridge-Knopoff model we can use our ability to follow the motion directly to take a closer look at the dynamics of individual events. A very large delocalized event is illustrated in Fig. 6. Here we show a sequence of configurations at equally spaced time intervals during the period in which slipping is actually taking place. The motion begins at the point labeled “epicenter” and looks initially like a localized event in which the blocks in a zone roughly of width $\tilde{\xi}$ slip forward irregularly. As the motion reaches the edges of the zone, it becomes a pair of smooth pulses that propagate outward at almost constant speed. Each nearly vertical line in Fig. 6 is a slipping region in which the blocks are jumping forward from one stuck configuration (the bottom curve) to another (the top). The right-moving pulse dies out quickly because it encounters a nearby region in which the blocks are firmly

²We have confirmed numerically that the delocalization length $\tilde{\xi}$ is proportional to ξ . However, the α dependence appears to be less strong than Eq. (4) would suggest. Tests of the weak logarithmic dependence on the additional parameters have not been carried out due to the limited ranges over which these parameters can be adjusted while maintaining good statistics.

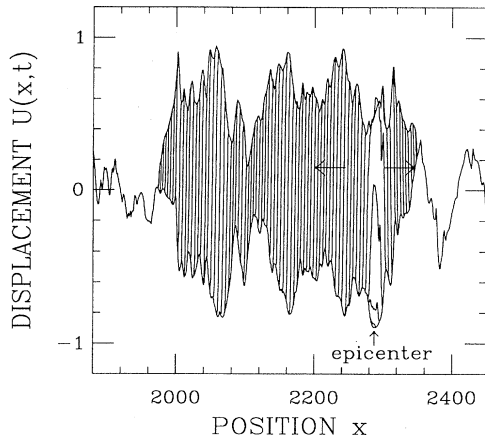


FIG. 6. The dynamics of an individual large event consist of narrow slipping pulses, which propagate at a speed of roughly ξ . New curves are drawn at equal time intervals during the event and represent the configuration at various stages between the initial configuration (bottom curve) and final configuration (top curve). The spatial variation of the pulse speed is apparent in the variation in spacing of the nearly vertical lines, which mark the slipping blocks. Lines that are relatively farther apart correspond to fast-moving pulses, which propagate through regions that are close to threshold, while the lines that are closer indicate a relatively slower speed, which occurs when the pulses pass through regions that are more stuck. It is interesting to note that, as a consequence of the large event, the configuration is nearly inverted: regions that were initially close to threshold slip further than regions that were initially far from threshold. Here we have taken $\xi/a=3$, $\alpha=1.2$, and $\sigma=0.01$.

stuck. The left-moving pulse, on the other hand, moves much farther, slowing slightly and then accelerating again as it passes through stuck regions, and finally coming to rest only after relieving the stress over a large portion of the fault.

Numerically we can follow the net motion forward as a function of time and, taking the Fourier transform of this, obtain the moment spectrum, a quantity that seismologists can measure. The spectra produced by the model exhibit power laws and are similar to spectra taken from the earth. Interestingly, ξ is again relevant. The model spectra for large events exhibit a bend at a frequency proportional to the inverse time required for a pulse to propagate a distance ξ (Shaw, 1993a).

Even more powerfully, analytic calculations have been made of the speed and shape of pulses propagating into a uniformly stuck state. The shape of slip pulses in the earth remains an open question, but one that is an important ingredient in the inversion process. Some simple considerations make it clear that even in our simple model this problem is nontrivial; indeed, just posing the problem leads us to explore some previously untouched but fundamental issues in fracture dynamics (Langer, 1992, 1993; Langer and Nakanishi, 1993). In the brief remarks that follow, we can provide only a very qualitative and nonrigorous summary of our ongoing investigations in this area. More details can be found in Langer and Tang (1991) and Myers and Langer (1993a).

Without loss of generality for these purposes, we can set $vt=0$ in Eq. (1) and, for simplicity, consider a pulse propagating into a system that is uniformly at, say, $U=-1+\epsilon$. Because the slipping threshold occurs at $\phi=1$, ϵ is our measure of distance from threshold; that is, it is the degree to which the system is stuck. Our problem is to find steady-state propagating solutions of the form $U(x,t)=U(x-vt)$ with $U(x \gg vt) \approx -1+\epsilon$, and to compute the speed v as a function of ϵ .

The simplest and most naive approach to this problem is to assume that the slipping friction $\phi(\dot{U} > 0)$ drops quickly to zero, in which case solutions of Eq. (1) have the form

$$U(x,t) \approx \begin{cases} 1-\epsilon, & \frac{x-vt}{\sqrt{v^2-\xi^2}} < -\frac{\pi}{2}, \\ -(1-\epsilon)\sin\left[\frac{x-vt}{\sqrt{v^2-\xi^2}}\right], & -\frac{\pi}{2} < \frac{x-vt}{\sqrt{v^2-\xi^2}} < \frac{\pi}{2}, \\ -1+\epsilon, & \frac{x-vt}{\sqrt{v^2-\xi^2}} > \frac{\pi}{2}. \end{cases} \quad (6)$$

Despite the fact that the slipping friction cannot be completely negligible at the onset of motion and at the resticking point, and despite the fact that we have written Eq. (6) without proper consideration of the boundary conditions at these points, this result turns out to be remarkably close to the actual behavior of the model. Formal steady-state solutions of properly posed interpretations of Eq. (1) can be shown to exist for a continuous range of supersonic speeds $v > \xi$; and the slipping motion, to a good approximation, is a free-slipping pulse

much like Eq. (6), whose width is proportional to $\sqrt{v^2-\xi^2}$. The numerical experiments, however, imply not a family of values of v , but precise selection independent of initial conditions.

The crucial, physically important fact about the velocity-selection problem is that its solution requires the introduction of a new length scale or, equivalently, a short-wavelength cutoff. We have dealt with this situation in two different ways. In our earliest work on this problem, we used the fact that the finite-difference ap-

proximation to Eq. (1), that is, the uniform block and spring model of Burridge and Knopoff, is perfectly well posed mathematically. For small block spacing a , a sufficiently accurate finite-difference correction can be obtained by adding the term $(\xi^2 a^2/12)\partial^4 U/\partial x^4$ to the right-hand side of Eq. (1). In recent investigations, we have preferred to add a viscous damping of the form $\eta\partial^2 \dot{U}/\partial x^2$ on the grounds that such a term has a more natural physical interpretation. This viscous term becomes $-\eta v\partial^3 U/\partial x^3$ when we look only for steady-state solutions. The relevant new length in this case is $\sqrt{\eta}$. Both techniques amount to adding a comparatively high derivative to the equation of motion, and thus introducing a singular perturbation that does in fact make the equation mathematically well defined. For simplicity, we shall refer here only to the finite-difference method, although it is the viscous model that has proved to be most interesting in a number of physical contexts.

With the addition of the singular perturbation and the associated new length scale, velocity selection in this system becomes a nonstandard version of an especially interesting class of dynamic phenomena. The history of work in this area goes back to the classic paper of Kolmogorov, Petrovskii, and Piscounov (1937) on front propagation in a nonlinear diffusion equation. In this case, we are dealing with a wave equation with a linear singular perturbation and an especially ferocious nonlinearity in the stick-slip friction. Nevertheless, the simplest version of the selection mechanism seems to be exactly correct for this system: the selected state is the one for which the steady-state solution is just on the margin of being unstable. While there remain some technical questions regarding the literal interpretation of this statement, its practical implementation has been checked by careful computations and found to be correct even, for example, for large block spacings in which the fourth-derivative approximation would be entirely inaccurate.

The results of this analysis are indicative of the interesting structure of the selection problem. We quote them only in the limit of small a and small "stuckness" parameter ϵ . The velocity is

$$\frac{v}{\xi} \approx 1 + \frac{1}{2} \left[\frac{3\alpha a}{2\xi} \right]^{2/3} \left[1 - \frac{\pi^2}{\ln^2(2\epsilon/3)} \right] \quad (7)$$

and the width of the pulse is

$$\Delta x \approx \sqrt{v^2 - \xi^2} \approx \xi \left[\frac{3\alpha a}{2\xi} \right]^{1/3}. \quad (8)$$

Note the following. In the continuum limit $a \rightarrow 0$, the velocity approaches the sound speed ξ from above and thus remains well behaved. The width Δx vanishes in this limit, but the number of blocks in it becomes infinite: $\Delta x/a \approx (\xi/a)^{2/3} \rightarrow \infty$. According to Eq. (7), the pulse slows with increasing ϵ . This is qualitatively consistent with the behavior seen in Fig. 6, where there is a clear deceleration as the pulse passes through regions where the original values of $U(x)$ are relatively large. At larger values of ϵ , where Eqs. (7) and (8) are no longer valid, v

falls below ξ . The pulses fail to propagate—the selected velocities vanish—at α -dependent values of ϵ that are always somewhat less than unity.

An especially interesting feature of the results reported in Myers and Langer (1993a) is that the selected pulses invariably probe the strongly nonlinear portion of the friction law (2). That is, the blocks slip as much as possible at speeds large enough that the friction is small.

The idea that the motion in very large earthquakes consists of narrow propagating slipping pulses has been advanced on the basis of observational data by Heaton (1990). Heaton's conjecture remains a basic open question and is the subject of considerable debate. Heaton's picture is supported robustly by our analytic and numerical studies. Our pulses are narrow in the sense that their thicknesses Δx are appreciably smaller than the "crust depth" ξ . Most remarkably, once they get started, our model pulses move steadily along the irregularly stressed fault, amplifying irregularities as they pass, but with no noticeable backscattering.

V. HIGHER DIMENSIONS: MOVING TOWARDS MORE REALISTIC MODELS

Certain intrinsic limitations of the one-dimensional Burridge-Knopoff model can be overcome by extending it to higher dimensions. For example, in the one-dimensional model, there are no elastic interactions between distant points on the fault, and there is no mechanism for radiative transport of elastic energy. In addition, real earthquakes have structure in the two-dimensional fault plane and, therefore, the scaling laws and exponents that we find in one dimension may not be the same as those in higher dimensions. Of course, the earth is three dimensional, but fully three-dimensional calculations analogous to those we have carried out for the one-dimensional model are still beyond the range of our computational capabilities. For this reason, our study of higher-dimensional models has begun with the consideration of two different two-dimensional models representing two orthogonal cross sections of the seismogenic zone.

First we consider a two-dimensional fault-plane model (Carlson, 1991b) in which the variable x , as before, describes position along the fault, and z is the depth below the surface. For simplicity, we consider displacements $U(x, z, t)$ only in the x direction. The equation of motion is

$$\tilde{U} = \xi^2 \nabla^2 U - U - \phi(\dot{U}, z) + vt, \quad (9)$$

which differs from Eq. (1) in the higher-dimensional gradient term, representing a two-dimensional lattice of coupling springs, and the depth dependence of the friction. In the simplest case, we have taken the friction to be independent of z . A more realistic option is to allow the friction to change with depth to account for the fact that friction in the earth depends on pressure and temperature.

Figure 7 is a typical magnitude vs frequency distribution for the fault-plane model. Comparing this with the corresponding results for the one-dimensional model (Fig. 5), we see that the scaling law describing small to moderately large events is remarkably unchanged; that is, the exponent $b=1$ in the Gutenberg-Richter relation (3) continues to hold. The most striking difference between the results in one and two dimensions is that, in two dimensions, the bump associated with large events is replaced by a relatively flat shoulder (which gives a somewhat better fit to the data). This occurs both with and without depth-dependent friction for systems that are sufficiently large. The bump reemerges, however, for faults that are sufficiently shallow (roughly for fault depths less than ξ). In fact, because the earth's crust is thin in comparison to the typical propagation length of a great earthquake, it is likely that the most realistic case is the relatively shallow two-dimensional fault with a depth of order ξ . In our simulations for both deep and shallow two-dimensional faults, there continues to be an excess of large events relative to the projected rate of smaller events. Of course, in two dimensions the crossover $\bar{\mu}$ will be modified because, according to dimensional analysis, it must scale like ξ^2 rather than ξ .

Results from the fault-plane model are qualitatively comparable to seismic reconstructions (Archuleta *et al.*, 1982) and depth-dependent measurements (Sibson, 1982). Figure 8 is an illustration of a moderately large event in the x - z plane. In Fig. 8(a) we show the blocks that are

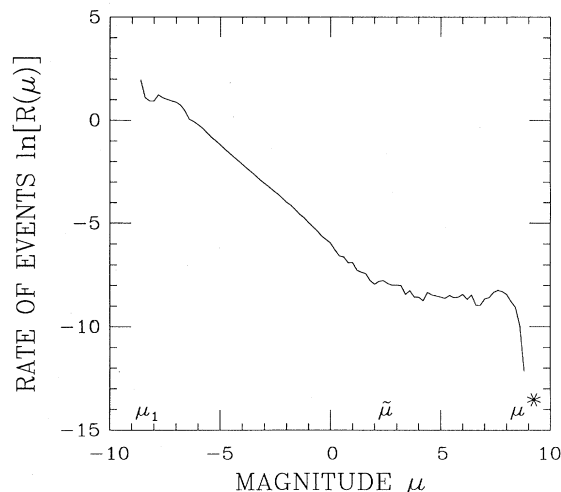


FIG. 7. Magnitude vs frequency distribution in the two-dimensional fault-plane model. Here we have taken $\sigma=0.01$, $\alpha=2.5$, $\xi/a=3$, $N_x=200$, and $N_z=100$. The results shown here are for depth-dependent friction. The corresponding distribution obtained when friction does not depend on depth is essentially identical. Interestingly, the exponent b in the Gutenberg-Richter law [Eq. (3)], which characterizes the distribution of smaller events, is the same here as it is in Fig. 5 for the one-dimensional model. In both cases we observe an excess of large events, though in sufficiently large two-dimensional systems it appears as a shoulder in the distribution (as in the case illustrated here) rather than as a bump.

slipping at equal time intervals. As in the one-dimensional model, we observe narrow propagating fronts. In this particular case, the event starts near the bottom of the fault and propagates both horizontally and vertically, sweeping out a slipping zone that is not at all radially symmetric or spatially uniform, as illustrated in the slip distribution shown in Fig. 8(b). In fact, in some cases we observe that the propagating fronts split and pass around regions that are firmly stuck. In the shallow-fault model, this splitting tends not to be observed and, instead, the slipping front spreads from bottom to top and then propagates unilaterally or bilaterally along the fault, again producing an irregular slip distribution.

Next we consider our second two-dimensional cross section of the earth, namely a crustal-plane model in which a one-dimensional fault (the x axis) is embedded in

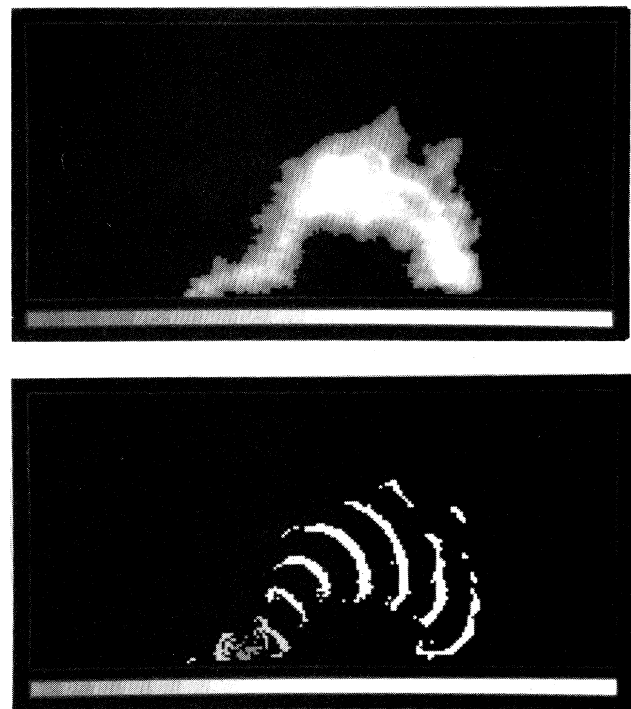


FIG. 8. A typical delocalized event in the two-dimensional fault-plane model (parameters as in Fig. 7). This event has $\mu=6$, which on the corresponding magnitude vs frequency distribution lies a little more than half of the way between $\bar{\mu}$ and the largest event μ^* . In this event 3522 of the 20 000 blocks were involved. The top figure illustrates the slip distribution during the particular event. Black corresponds to no slip, while the grey-to-white scale ranges linearly up to the maximum displacement during the event. The bottom figure illustrates the slipping blocks at equal intervals of time, grey corresponding to early times and white corresponding to the latest times during the event. As in one dimension, large events consist of narrow propagating fronts. However, by studying the two-dimensional model, more direct comparisons can be made with seismic reconstructions of actual events. These reconstructions suggest that complex rupture patterns, similar to that shown here, are generated by real earthquakes.

a two-dimensional elastic medium (the x - y plane) (Langer, 1993; Langer and Nakanishi, 1993; Myers and Langer, 1993b). Again, for simplicity, we consider only a one-component displacement field $U(x, y, t)$, and we assume that U satisfies a wave equation with a linear driving force:

$$\ddot{U} = \xi^2 \nabla^2 U - U + vt. \quad (10)$$

In analogy to Eqs. (1) and (9), the term $(-U + vt)$ in Eq. (10) describes elastic coupling of a seismogenic layer of thickness ξ to a stable lower region of the crust. The stick-slip friction between the two sides of the fault is part of the boundary condition that specifies the stress $\partial U / \partial y$ at $y=0$:

$$\left. \frac{\partial U}{\partial y} \right|_{y=0} = \phi(\dot{U}) - \eta \left. \frac{\partial^2 \dot{U}}{\partial x^2} \right|_{y=0}. \quad (11)$$

Note that we have included the viscous damping mentioned in Sec. IV as the second part of the traction on the right-hand side of Eq. (11). This term has the effect of smoothing the system at the smallest length scales and thus assuring that Eqs. (10) and (11) are well posed mathematically.

Some recent studies of models of this kind have focused on the case in which the stick-slip friction $\phi(\dot{U})$ in Eq. (11) is replaced by a cohesive stress that depends upon displacement rather than slipping speed. The resulting model describes ordinary crack propagation with a nonzero fracture energy rather than unstable rupture on an existing fault. It has some extremely interesting properties, in particular, a dissipation-dependent threshold for the onset of rapid motion. The important com-

mon feature of both versions of the model is that they accurately include stress concentration at the crack tip or rupture front. This feature is completely absent in the one-dimensional models, and there is every reason to expect that it should have a qualitative effect on the dynamics of the system. Indeed, it is the combination of two-dimensional stress concentration and viscous dissipation on the crack face that produces the interesting properties of the fracture model.

So far, studies of this crustal-plane model in earthquake mode (primarily by C. Myers) have focused on issues related to pulse propagation in analogy to the one-dimensional studies described in Sec. IV. Myers has obtained convincing numerical evidence that large-scale slipping occurs in this model via a mechanism ostensibly identical to the Heaton pulse; the system resticks behind the rupture front, and the width of the slipping zone is relatively narrow (Myers and Langer, 1993b). A picture of one of these pulses is shown in Fig. 9. The major outstanding question is whether this model is intrinsically chaotic and, if so, whether the earthquakelike events have magnitudes that are distributed according to something like the Gutenberg-Richter law.

VI. PREDICTABILITY: FORECASTING THE NEXT LARGE EARTHQUAKE

One of the main goals of seismology is to develop better algorithms and more sensitive probes to aid in predicting large earthquakes. The problem of earthquake prediction is extremely complex. Our knowledge of the detailed structure of subsurface fault zones remains re-

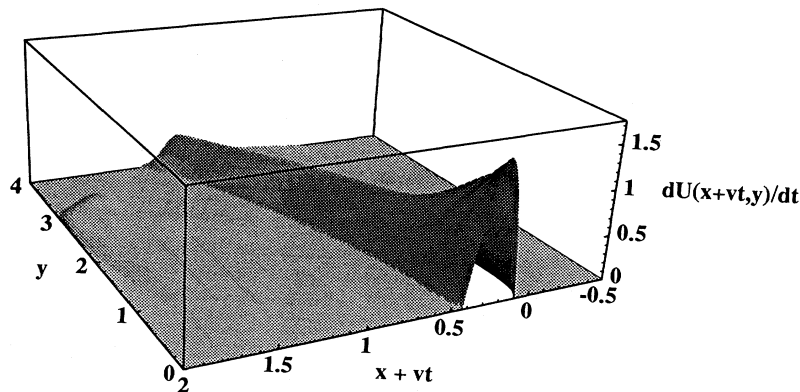


FIG. 9. Snapshot of the slip rate $\dot{U}(x + vt, y)$ in the two-dimensional crustal-plane model, demonstrating the existence of a “self-healing pulse of slip.” The fault lies along the line $y=0$, and the snapshot is taken in a comoving frame of velocity $-v$, where $v=1$ is the steady-state velocity for this particular pulse. The pulse is propagating to the right along the $x + vt$ axis. The model parameters are $\alpha=3.0$, $\eta=0.1$. A first-order implicit finite-difference integration has been carried out on a rectangular grid of 250×100 points (with $\Delta x=0.01$, $\Delta y=0.05$), although only 80 points are shown in the y direction. The boundaries are free (zero derivative boundary conditions) along all edges except $y=0$, where the fault traction is specified by the model. An artificial viscous zone is introduced for $y > 4.5$ in order to minimize reflections from the back boundary. In this zone, an extra viscous term of the form $\eta(y)\nabla^2(\dot{U})$ is added to the bulk equation of motion, with $\eta(y)$ growing smoothly from zero.

markably incomplete, and we have been collecting accurate information about seismic activity only for a few decades—much less than a single loading period for most fault segments. In addition, earthquakes show symptoms of being intrinsically chaotic phenomena.

The study of dynamical models may be particularly useful in a situation of this kind. Models are not limited by geological time scales; for example, our computer simulations span the equivalent of hundreds of loading periods with perfect detection of events. Furthermore, the uniform Burridge-Knopoff model that we study is a particularly good candidate for such investigations because it is deterministically chaotic, making it impossible to predict detailed behavior far into the future. Yet this model, realistically, possesses a characteristic loading time, a distinction between small and large events, and a tendency—quite apparent in Figs. 4 and 10—for clusters of small events to be correlated with the onset of large ones. Thus it seems interesting to inquire about the extent to which it is possible, using only the analogs of techniques that are available in the real world, to predict the times and locations of large events in this model.

The seismological literature refers to three categories of earthquake hazard assessments: long-term, intermediate-term, and short-term predictions. Long-term predictions are estimates of earthquake probability made roughly on the scale of tens of years (WGCEP, 1988). Such assessments are used in establishing building codes and, especially, in siting sensitive facilities such as nuclear reactors. They generally are based on estimates of recurrence times for the large events on major active faults and on whatever other geological information might be available.

In contrast, intermediate-term predictions are made on time scales of years, and short-term predictions on scales of days. The hope is that some more detailed information regarding the local state of the system, perhaps based on patterns of small events, may ultimately be used to provide early warnings of imminent large events. Thus there is much interest in learning how to make intermediate- and short-term predictions in a reliable way. One major contribution in the area of intermediate-term prediction has been made by Keilis-Borok *et al.* (1990), Keilis-Borok and Kossobokov (1990), and Keilis-Borok and Rotwain (1990), who have developed a set of prediction algorithms using relatively simple pattern recognition techniques. However, because of the sparsity of real seismic data, it has been difficult to evaluate the quality of these algorithms. One purpose of our work has been to estimate the intrinsic uncertainties and the prospects for more accurate results by finding out how well such algorithms can be made to work for uniform Burridge-Knopoff models (Pepke *et al.*, 1993).

The goal of intermediate-term earthquake prediction as formulated by Keilis-Borok *et al.* is considerably more limited than the term might seem to imply. One is not actually trying to predict earthquakes ten years in advance. Rather, the idea is simply to recognize patterns of seismic activity that might indicate times of increased

probability—the so-called TIPs—for major earthquakes. The goal is to make these alarms as accurate as possible. The times during which these are “on” should be short and the geographical regions to which they apply should be small, and yet they should “capture” almost all of the major seismic events with few, if any, false alarms. Given this statement of the problem, it is relatively easy to define mathematically significant measures of success and to use those measures to test various algorithms, that is, to evaluate various criteria for turning on the TIPs.

In the pattern recognition algorithms of Keilis-Borok *et al.*, TIPs are determined by keeping track of as many as eighteen different seismicity-based precursors, such as an increase in activity or an increase in the rate of aftershocks. The strategy is to use computer-based pattern recognition techniques to identify various combinations of precursory behavior that, with high probability, indicate that a major event is imminent. In the real world, no single precursor appears to be capable of forecasting all large events. The best single precursors can capture roughly half of the large events but need to turn on alarms at least 20% of the recurrence interval in order

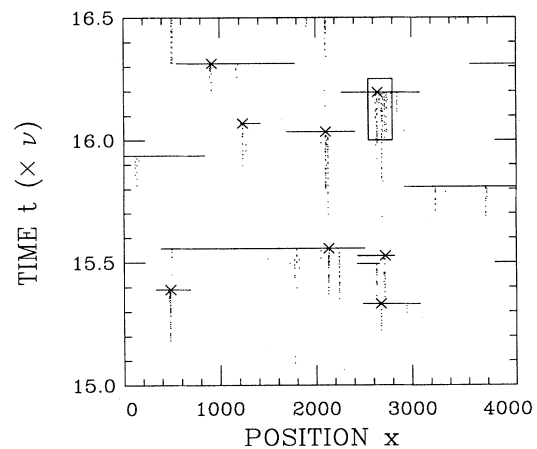


FIG. 10. A sample catalog illustrating the events that take place as a function of position and time. Similar to the sequence of events illustrated in Fig. 4, there the lowest contour (a line segment) marks the first event, and subsequent curves correspond to integration of Eq. (1) forward in time. In this case we forego illustrating the displacement, and instead explicitly plot time on the vertical axis, measured relative to the inverse loading speed, so that values on that axis represent $t\nu = \delta U$, i.e., the net displacement of initially adjacent points on opposite sides of the fault. A line segment is drawn through all of the blocks that slip during an event, and a cross marks the position of the epicenter of each large event. The clustering of small events in the local minima in Fig. 4 corresponds here to the trails of short line segments, which end at the longer segments, i.e., large events. The box corresponds to a space-time window within which the precursory measures, such as activity or active zone size, which are used in the intermediate-term prediction algorithms are evaluated. The data are taken from a simulation in which $\sigma = 0.01$, $\alpha = 3$, $\xi/a = 10$, and $N = 8192$, though only a fraction of the system is shown.

to do so. When combinations of seven or more precursors are used, the success rate goes to about 80%, but with the same, relatively poor, time resolution.

The patterns of activity that precede large events in the uniform Burridge-Knopoff model are much simpler than in the real world; thus we expect the pattern recognition algorithms to be comparatively more successful. In particular, almost every large event in the model is preceded by a marked increase in activity, i.e., the rate of small events, in the neighborhood of the future epicenter (Shaw *et al.*, 1992). This is illustrated in Fig. 10, which, like Fig. 4, illustrates a typical sequence of events. In this case, the time of occurrence of each event appears explicitly, and each event is marked by a line drawn through the blocks that slip. For large events, a cross marks the position of the epicenter, which is clearly correlated with precursory activity. However, the duration of this activity is relatively long—about one third of the entire repeat time on average. Moreover, there is large variability in the overall amplitude of the precursory activity and in the time prior to the large event at which it starts. Thus the question remains: to what extent is this precursory activity useful for making predictions on the time scales (a small fraction of the mean repeat time) that are useful for intermediate-term forecasts?

To answer this question, we have considered the simplest versions of the pattern recognition algorithms, that is, algorithms based on single precursors. We find that with most precursors, such as the total activity, we can predict roughly 90% of the events with alarm times of the order of 15%–25% of the seismic cycle. This is somewhat better than Keilis-Borok *et al.*'s real-world experience, but not dramatically so. Interestingly, there is one exception to this. We have found a new precursor, not previously used by seismologists, that leads to significantly more accurate predictions in the Burridge-Knopoff model. The definition of this new precursor, which we call "active zone size," is related to the concept of the delocalization length ξ . With it we can predict 90% of the large events with TIPs that are "on" only during 5% of the recurrence interval.

"Active zone size" is the spatial extent of small-scale seismicity. In a space-time window such as that illustrated in Fig. 10, the active zone size is defined to be the total number of blocks that have slipped, regardless of how many times. As the time of a large event approaches, the active zone grows, leading to the development of a triggering region of size ξ for the nucleation of a large event, as described in Sec. IV. Since nearly all of the accumulated stresses are relieved in the large events, the small events serve primarily as indicators that the system is locally poised near the threshold of instability. While the total number of events (i.e., activity) is clearly not an independent measure of the status of the system, it is a much less sensitive probe than active zone size of the size of the region that is close to threshold. It remains to be seen whether or not this new measure will aid in efforts

to predict large events in the earth.

Many questions pertaining to the use of models in the development and testing of earthquake prediction algorithms are still unanswered. One of these is the extent to which algorithms may be improved by combining multiple precursors as is done by Keilis-Borok and colleagues. We currently are studying this question and, so far, find that such techniques do not lead to substantial gains in the Burridge-Knopoff model. In fact, it is not immediately clear to what extent even comparatively sophisticated techniques might be successful if based only on information contained in our catalogs of seismic events. More accurate predictions may require information about other phenomena, such as aftershocks, which are very common for crustal earthquakes, but which do not occur in our current version of the model. We hope to add aftershocks to a more realistic, future version of the model (Shaw, 1993b). Because the uniform Burridge-Knopoff model is fully deterministic, arbitrarily accurate predictions would be possible if more detailed information about the configuration of the system could somehow be obtained. For example, we would like to test the possibilities of combining seismicity data with the analog in the model of geological information about local displacements or stresses. It is this kind of investigation that we suspect may lead to the most significant practical applications of the work done in this project.

ACKNOWLEDGMENTS

We should especially like to thank our collaborators, who made important contributions to the work presented here: C. Tang, C. Myers, S. Pepke, and H. Nakanishi. We should also like to thank T. Hanks for useful comments on the manuscript. The work of J.M.C. was supported by a grant from the Alfred P. Sloan Foundation, a fellowship from the David and Lucile Packard Foundation, NSF grant DMR-9212396, and an INCOR grant from the CNLS at Los Alamos National Laboratories. The work of J.S.L. was supported by DOE grant DE-FG03-84ER45108. The work of B.E.S. was supported by the Southern California Earthquake Center grant USC-572726, and USGS grant 1434-93-G-2284. The work of J.M.C., J.S.L., and B.E.S. was also supported by NSF grant PHY89-04035.

REFERENCES

- Archuleta, R. J., E. Cranswick, C. Mueller, and P. Spudich, 1982, *J. Geophys. Res.* **87**, 4595.
- Bak, P., C. Tang, and K. Wiesenfeld, 1987, *Phys. Rev. Lett.* **59**, 381.
- Barriere, B., and D. L. Turcotte, 1991, *Geophys. Res. Lett.* **18**, 2011.
- Burridge, R., and L. Knopoff, 1967, *Bull. Seismol. Soc. Am.* **57**, 3411.
- Carlson, J. M., 1991a, *J. Geophys. Res.* **96**, 4255.

- Carlson, J. M., 1991b, *Phys. Rev. A* **44**, 6226.
- Carlson, J. M., and J. S. Langer, 1989a, *Phys. Rev. Lett.* **62**, 2632.
- Carlson, J. M., and J. S. Langer, 1989b, *Phys. Rev. A* **40**, 6470.
- Carlson, J. M., and J. S. Langer, B. E. Shaw, and C. Tang, 1991, *Phys. Rev. A* **44**, 884.
- Chen, K., P. Bak, and S. Obukov, 1991, *Phys. Rev. A* **43**, 625.
- Davison, F. C., Jr., and C. H. Scholz, 1985, *Bull. Seismol. Soc. Am.* **75**, 1349.
- Glatzmaier, G. A., G. Schubert, and D. Bercovici, 1990, *Nature* **347**, 274.
- Gutenberg, B., and C. F. Richter, 1954, *Seismicity of the Earth and Associated Phenomena* (Princeton University, Princeton, NJ).
- Hanks, T. C., 1992, *Science* **256**, 1430.
- Hanks, T. C., and H. Kanamori, 1979, *J. Geophys. Res.* **84**, 2348.
- Heaton, T. H., 1990, *Phys. Earth Planet. Inter.* **64**, 1.
- Kagan, Y. Y., 1982, *Geophys. J. R. Astr. Soc. Can.* **71**, 659.
- Keilis-Borok, V. I., and V. G. Kossobokov, 1990, *Phys. Earth Planet. Inter.* **61**, 73.
- Keilis-Borok, V. I., L. Knopoff, V. G. Kossobokov, and I. Rotwain, 1990, *Geophys. Res. Lett.* **17**, 1461.
- Keilis-Borok, V. I., and I. M. Rotwain, 1990, *Phys. Earth Planet. Inter.* **61**, 57.
- Knopoff, L., 1993, unpublished.
- Kolmogorov, A., I. Petrovsky, and N. Piscounov, 1937, *Bull. Univ. Moscow Ser. Int., Sec. A* **1**, 1.
- Langer, J. S., 1992, *Phys. Rev. A* **46**, 3123.
- Langer, J. S., 1993, *Phys. Rev. Lett.* **70**, 3592.
- Langer, J. S., and H. Nakanishi, 1993, *Phys. Rev. E* **48**, 439.
- Langer, J. S., and C. Tang, 1991, *Phys. Rev. Lett.* **67**, 1043.
- Myers, C. R., and J. S. Langer, 1993a, *Phys. Rev. E* **47**, 3048.
- Myers, C. R., and J. S. Langer, 1993b, unpublished.
- Nishenko, S. P., and R. Buland, 1987, *Bull. Seismol. Soc. Am.* **77**, 1382.
- Pacheco, J. F., C. H. Scholz, and L. R. Sykes, 1992, *Nature* **235**, 71.
- Pepke, S. L., J. M. Carlson, and B. E. Shaw, 1993, *J. Geophys. Res.* (in press).
- Sahimi, M., M. C. Robertson, and C. G. Sammis, 1993, unpublished.
- Scholz, C. H., 1990, *The Mechanics of Earthquakes and Faulting* (Cambridge University, New York).
- Schwartz, D. P., and K. J. Coppersmith, 1984, *J. Geophys. Res.* **89**, 5681.
- Shaw, B. E., 1993a, *Geophys. Res. Lett.* **20**, 643.
- Shaw, B. E., 1993b, *Geophys. Res. Lett.* **20**, 907.
- Shaw, B. E., J. M. Carlson, and J. S. Langer, 1992, *J. Geophys. Res.* **97**, 479.
- Sibson, R. H., 1982, *Bull. Seismol. Soc. Am.* **72**, 151.
- Vasconcelos, G. L., M. S. Vieira, and S. R. Nagel, 1992, *Physica A* **191**, 69.
- Wesnousky, S. G., 1993, unpublished.
- Working Group on California Earthquake Prediction (WGCEP), 1988, U.S. Geol. Surv. Open File Report No. 88-398.

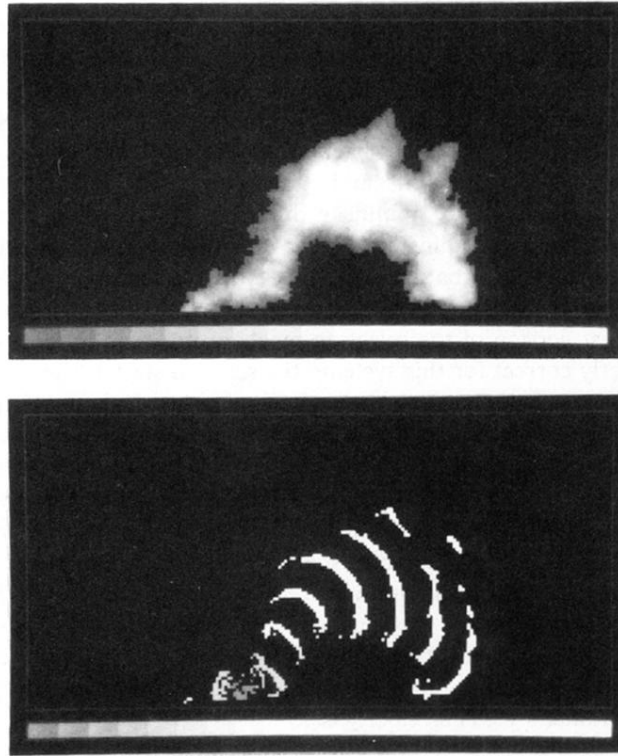


FIG. 8. A typical delocalized event in the two-dimensional fault-plane model (parameters as in Fig. 7). This event has $\mu=6$, which on the corresponding magnitude vs frequency distribution lies a little more than half of the way between $\bar{\mu}$ and the largest event μ^* . In this event 3522 of the 20 000 blocks were involved. The top figure illustrates the slip distribution during the particular event. Black corresponds to no slip, while the grey-to-white scale ranges linearly up to the maximum displacement during the event. The bottom figure illustrates the slipping blocks at equal intervals of time, grey corresponding to early times and white corresponding to the latest times during the event. As in one dimension, large events consist of narrow propagating fronts. However, by studying the two-dimensional model, more direct comparisons can be made with seismic reconstructions of actual events. These reconstructions suggest that complex rupture patterns, similar to that shown here, are generated by real earthquakes.